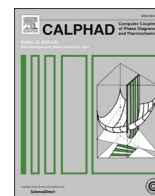




Contents lists available at ScienceDirect

Calphad

journal homepage: www.elsevier.com/locate/calphad

Rheological properties of $\text{Al}_2\text{O}_3\text{-CaO-SiO}_2$ slags

Kai Tang^{a,*}, Casper van der Eijk^a, Sylvain Gouttebroze^b, Qiang Du^b, Jafar Safarian^c, Gabriella Tranell^c

^a SINTEF Industry, N-7465, Trondheim, Norway

^b SINTEF Industry, N-0314, Oslo, Norway

^c Department of Materials Science and Engineering, Norwegian University of Science and Technology, Trondheim, Norway

ARTICLE INFO

Keywords:

$\text{Al}_2\text{O}_3\text{-CaO-SiO}_2$

Viscosity

Phenomenological model

Vogel-Fulcher-Tammann formalism

TTT

CCT

ABSTRACT

The $\text{Al}_2\text{O}_3\text{-CaO-SiO}_2$ ternary is a basic oxide system relevant for the Pedersen alumina production process and for aluminothermic silicon production with low environmental impact using secondary aluminium and silica raw materials. Rheological property is one of the most important properties for the above applications. A phenomenological viscosity model, inspired by the Calphad technique, has been proposed for the description of the rheological properties covering from homogenous liquid to heterogenous partial solidified $\text{Al}_2\text{O}_3\text{-CaO-SiO}_2$ slags. The model has been developed by modification of the well-known Vogel-Fulcher-Tammann (VFT) formalism. Based on the phenomenological viscosity model, the effective diffusivity of slag can be evaluated. The relationships between cooling temperature rate, incubation time of solid precipitates as well as transition temperature have then been estimated. The model calculated the isothermal time-temperature-transformation (TTT) and the non-isothermal continuous-cooling-transformation (CCT) curves of CaAl_2O_4 and anorthite phases are in good agreement with the experimental observations.

1. Introduction

Slag is one of the engineering important materials for many important applications. It is primarily used in metallurgical processes for removing impurity elements from the metal phase, protecting the hot metal from oxidation, and lubricating between the mold and metal strand during continuous casting. In order to improve the sustainability of the metal industry and alleviate the environmental impact, the valorization of slag has received wide attention from the scientific and engineering communities.

The fundamental study of slag solidification has attracted significant attention in the past decades, including optimization of the microstructure of slag product [1], recover heat energy from the hot slag [2, 3], freeze linings formation to protect the refractory walls in pyro-metallurgical processes [4] and continuous casting mold fluxes optimization [5]. In the production of alumina via the Pedersen process [6,7] and high- TiO_2 ilmenite [8], slag is the main product, whereas pig iron metals become the by-products. The necessity of fundamental investigation for the solidification characteristics of the slags is indisputable and obvious. However, there is still a lack of theoretical and experimental studies to understand the evolution of slag structure in

solidification.

The viscosity of slag is one of the key parameters for the mathematical description of the slag solidifications as well as the impact on the kinetics of chemical reactions. The presence of suspended solid seriously affects the viscosity of silicate melts, as indeed it affects the viscosity of any other type of melt. Near the glass transition temperature, the viscosity increases continuously but rapidly with cooling. As the glass forms, the molecular relaxation time increases with an Arrhenius-like form in some liquids but shows highly non-Arrhenius behaviour in others. The formers are said to be 'strong' liquids, and the latter 'fragile' liquids [9]. The non-Newtonian behaviour is commonly observed in crystal-melt slushes at concentrations higher than a certain limit, the measurement signal will be disturbed by the interference of solid particles.

Great efforts have been made to study the effect of the fraction, shape and size of the solid particles on the viscosity of various suspensions. Numerous viscosity models have been established to correlate the apparent viscosity and solid fraction, as summarized by Vargas et al. [10] However, the existing models take only the solid fraction into consideration. Since the shape and size distribution of solid particles play a significant role in the rheological properties of heterogenous

* Corresponding author.

E-mail address: kai.tang@sintef.no (K. Tang).

<https://doi.org/10.1016/j.calphad.2022.102421>

Received 6 July 2021; Received in revised form 1 March 2022; Accepted 20 March 2022

Available online 27 March 2022

0364-5916/© 2022 The Authors. Published by Elsevier Ltd. This is an open access article under the CC BY license (<http://creativecommons.org/licenses/by/4.0/>).

melts, a universally valid viscosity model has so far not been proposed. In addition, it is difficult to real-time determinate the fraction, shape, and size distribution of solids in the solidification process.

In order to control the Al_2O_3 -CaO based slags in the new alumina production process¹ and Al_2O_3 -SiO₂ based slags for silicon production with low environmental impact using secondary aluminium and silica raw materials², the rheological properties of Al_2O_3 -CaO-SiO₂ slags have been the subject of the present study. A phenomenological viscosity model, inspired by the Calphad technique, has been proposed for the description of the rheological properties covering from homogeneous liquid to heterogeneous partial solidified Al_2O_3 -CaO-SiO₂ slags. The model has been developed by modification of the well-known Vogel-Fulcher-Tammann (VFT) formalism. Based on the phenomenological viscosity model, the effective diffusivity of slag can be evaluated. The relationships between cooling temperature rate, incubation time of solid precipitates as well as transition temperature have then been estimated.

2. Phenomenological model

As mentioned in the previous section, the existing viscosity models, including Iida et al. [11], Riboud et al. [12] and our early viscosity model [13], are all developed based mainly on the two-parameter Arrhenius relationship. Modifications are generally taken place by expanding the Arrhenius coefficients as composition- and temperature-dependent parameters. Although the viscosity models based on microstructure units of molten slag [13–15] have certain advantages in predicting the viscosity of multicomponent silicate melts with scattered or missing experimental data, these models work poorly for the viscosity of heterogeneous silicates.

For the heterogeneous silicate mixtures, numerous attempts have been made to model the viscosity of particle-containing dilute suspensions as well as dense slurries. As reviewed by Vargas et al. [10], most of the models treated solids as spheres. In some cases, the irregular solids were simply treated as ellipsoids characterized by the ratio of the long axis to the short axis. By examining about 5000 more experimental data, they concluded that simple models exist which can give an indication of the overall viscosity of the heterogeneous silicates if the solid fraction and their shape are known. Costa [16] demonstrated the examples of simple mathematic model for the high solid fraction melts.

The Vogel [17]-Fulcher [18]-Tammann [19] (VFT) semi-empirical equation has been widely used in evaluating the viscosities of silicate systems. It has also been recognised recently by Mauro et al. [20], who proposed a new model, that the VFT equation is the most popular viscosity model. The VFT equation is generally accepted to give an adequate representation of the temperature dependence of silicate melts [10]. It uses three adjustable parameters to describe the viscosity of liquids as a function of temperature, and especially for strongly temperature dependent variation in the supercooled regime [21]. It fits generally well with the experimental results for silicates at temperatures above liquidus as well as the supercooled liquids. Although many authors have tried to give a physical picture of the VFT equation, there is no rigorous theoretical derivation of the equation. We therefore define the VFT equation as a phenomenological viscosity model.

The original VFT equation is not an adequate representation of both the temperature and composition dependences of the viscosities for an entire ternary system. Attempt to expanding the parameters as temperature and composition dependencies has been made by one of the present authors. The modified VFT equation has successfully applied to describing the viscosities of the TiO_2 -FeO- Ti_2O_3 ternary system applicable to the high-titania slag system in broad composition and temperature ranges, including the solid-liquid heterogeneous regime [22]. The

average relative error between the viscosity calculation results by modified VFT equation and experimental data is less than 18.8%, which is lower than the experimental uncertainties of $\pm 25\%$ [23].

The viscosities of both homogeneous liquid and heterogeneous partial solidified Al_2O_3 -CaO-SiO₂ slags has in this work been expressed by the following modified VFT equation:

$$\log \eta(T, x) = \log \eta_\infty(x) + \frac{A(T, x)}{T - T_0(T, x)} \quad (1)$$

where η denotes viscosity in Pa-s, T is the temperature in K, x is composition in molar fraction. Inspired by the Calphad modelling on the excess properties of the liquid phase, the pre-exponential factor, $\log \eta_\infty(x)$, is expressed as the composition-dependent in the present work. The other two VFT parameters are expanded as both the composition- and temperature-dependent. In fact, $T_0(T, x)$ defines the temperature at which viscosity approach to infinite, while parameter $A(T, x)$ corresponds to the pseudo activation energy associated with the viscous flow. It is thought to represent a potential energy barrier obstructing the structural rearrangement of the slag [24]. Consequently, the above parameters are written as:

$$A = \lg \eta_\infty(x) = \sum_{i=1}^n r_i x_i \quad (2)$$

$$B = A(T, x) = \sum_{i=1}^n \sum_{j=1}^m [x_i x_j (a_{ij} + b_{ij} T)] \quad (3)$$

$$C = T_0(T, x) = \sum_{i=1}^n \sum_{j=1}^m [x_i x_j (c_{ij} + d_{ij} T)] \quad (4)$$

where 1 refers SiO₂, 2 for Al₂O₃ and 3 denotes CaO. For ternary Al_2O_3 -CaO-SiO₂ slag, $n = m = 3$ in above equations. It is generally accepted that the parameters of viscosity models could be fitted with multiple non-linear regression algorithms. The Excel Solver Add-In has been used to fit the model parameters using experimental viscosity data.

The experimental viscosity data of Al_2O_3 -CaO-SiO₂ slags were compiled in the second edition of the Slag Atlas in 1995 [23]. Since 1995, there have been many authors who reported the viscosities in this ternary slag system [25–30]. Approximately 1192 viscosity data points reported in the literature have been collected. The experimental viscosity data in the literature and used in the present investigation are

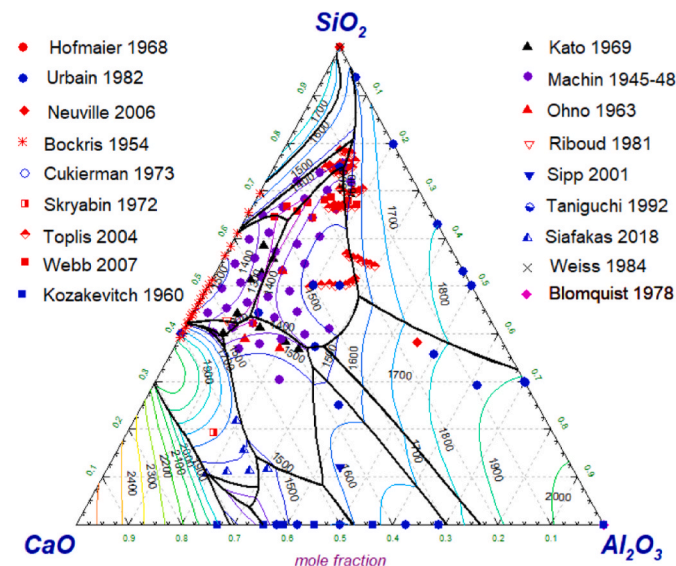


Fig. 1. The experimental viscosity data and their distribution in an Al_2O_3 -CaO-SiO₂ triangular coordinate.

¹ <https://www.ensureal.com/>.

² <https://www.sisal-pilot.eu/>.

shown in the $\text{Al}_2\text{O}_3\text{-CaO-SiO}_2$ triangular coordinate in Fig. 1. The iso-liquidus temperature and primary crystallized phases in the $\text{Al}_2\text{O}_3\text{-CaO-SiO}_2$ system were calculated using the FactSage commercial database [31]. Generally speaking, most of the experimental viscosity data cover the liquid phase at the temperature range below 1700 °C. Few measurements for pure SiO_2 and Al_2O_3 were also reported [32–35]. No direct viscosity measurement for pure CaO. The experimental data for $\text{SiO}_2\text{-CaO}$ and $\text{Al}_2\text{O}_3\text{-CaO}$ binary, as well as $\text{Al}_2\text{O}_3\text{-CaO-SiO}_2$ ternary slags with lower melting temperatures, are rather rich than those in the $\text{Al}_2\text{O}_3\text{-SiO}_2$ binary slag.

3. Results and discussion

The viscosities of $\text{Al}_2\text{O}_3\text{-CaO-SiO}_2$ silicate slags in both the homogenous and heterogenous regimes have been modelled by fitting the modified VFT parameters shown in Fig. 1. The model parameters are listed in Table 1.

Fig. 2 shows a comparison of the modified VFT modelling calculations with the original experimental data. The model can reproduce the experimental viscosity data over a wide temperature range. Generally, the threshold of viscosity at the glass-transition temperature, T_g , is 10^{12} Pa s. Obviously, the present modified VFT equation is able to calculate the viscosities of $\text{Al}_2\text{O}_3\text{-CaO-SiO}_2$ slags to the glass-transition supercooled regime. This provides a sound basis for the further application of the present viscosity model in the simulation of the solidification of the $\text{Al}_2\text{O}_3\text{-CaO-SiO}_2$ slags.

Fig. 3 shows the calculated viscosities for six low- SiO_2 content $\text{Al}_2\text{O}_3\text{-CaO-SiO}_2$ slags as a function of temperature. The corresponding experimental values measured by Siafakas et al. [27,28] are superimposed for the verification. Siafakas et al. determined the viscosities of six $\text{Al}_2\text{O}_3\text{-CaO-SiO}_2$ slags by aerodynamic levitation (for $T > 2229\text{K}$ in the homogenous liquid range) and rotating bob (for $T < 1898\text{K}$ in the partial solidified range) [27,28]. They also used six different Mauro equations [20,36] to fit their measurements [28], respectively. The current model, using only one set of the model parameters, can reproduce the sharp super-Arrhenius behaviour of the supercooled $\text{Al}_2\text{O}_3\text{-CaO-SiO}_2$ slags.

Fig. 4 shows the calculated iso- $\log\eta$ contours of the binary $\text{Al}_2\text{O}_3\text{-SiO}_2$ and $\text{Al}_2\text{O}_3\text{-CaO}$ slags by the present modified VFT model. The corresponding 3d-plot for the composition-temperature-viscosity relations in $\text{Al}_2\text{O}_3\text{-SiO}_2$ and $\text{Al}_2\text{O}_3\text{-CaO}$ binary slags are shown in the diagram. The liquidus of $\text{Al}_2\text{O}_3\text{-SiO}_2$ and $\text{Al}_2\text{O}_3\text{-CaO}$ slags are also superimposed in Fig. 4(a) and (c). The ability of the modified VFT equation in evaluations of both the homogeneous and heterogeneous slags is demonstrated. Toplis and Dingwell [29] measured 44 viscosities of $\text{Al}_2\text{O}_3\text{-CaO-SiO}_2$ slags. They found that the most prominent feature in this ternary system is a viscosity maximum roughly with a ridge along the Pseudo-binary $\text{SiO}_2\text{-CaAl}_2\text{O}_4$. Grundy et al. [14] thus introduced a fictional associate, CaAl_2O_4 , in their modelling of the viscosity of $\text{Al}_2\text{O}_3\text{-CaO-SiO}_2$ slag, in order to reproduce the pronounced viscosity maxima in this ternary system. The present model also gives the pronounced viscosity maxima in the middle of $\text{Al}_2\text{O}_3\text{-SiO}_2$ binary system. This provides the reproduction of viscosity maximum in the middle

Table 1

The modified VFT parameters for the $\text{Al}_2\text{O}_3\text{-CaO-SiO}_2$ slags.

r_1	r_2	r_3			
-7.375	-3.123	-4.34			
a_{11}	a_{22}	a_{33}	a_{12}	a_{13}	a_{23}
26670	3328	2890	67018	-21726	-7867
b_{11}	b_{22}	b_{33}	b_{12}	b_{13}	b_{23}
0	0	0	-15.8	29.6	2.46
c_{11}	c_{22}	c_{33}	c_{12}	c_{13}	c_{23}
-24.63	-429	-770	-5123	-8298	-792
d_{11}	d_{22}	d_{33}	d_{12}	d_{13}	d_{23}
0	0	0	4.88	7.35	-2.45

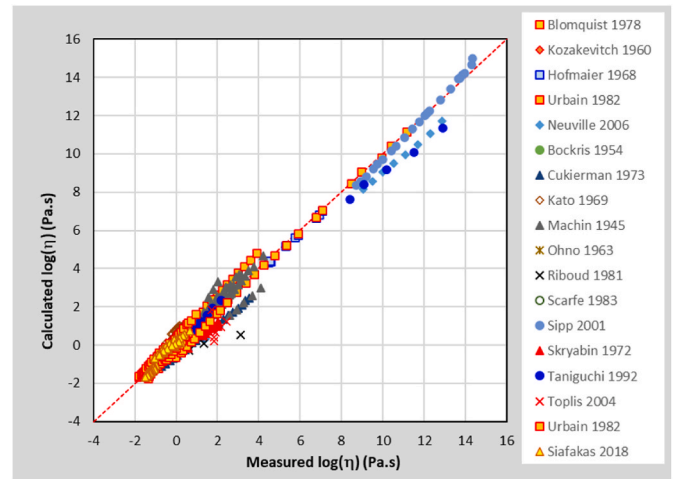


Fig. 2. Comparison of the calculated viscosities of $\text{Al}_2\text{O}_3\text{-CaO-SiO}_2$ with the experimental data.

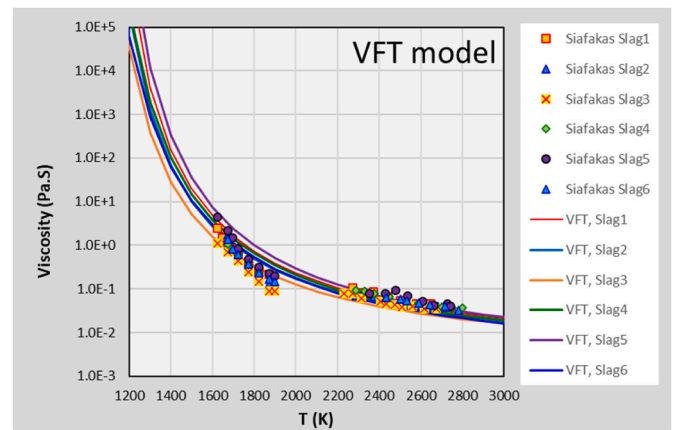


Fig. 3. The viscosities of low- SiO_2 $\text{Al}_2\text{O}_3\text{-CaO}$ slags modelled by modified VFT equation.

ridge of the ternary slags.

Obviously, the modified VFT equation given by Eq. (1) is readily extended to calculate the viscosities of the higher-order oxide systems. For multicomponent oxide systems, like the Calphad method, quaternary and higher-order parameters are generally rather small, and they can be neglected. Thus, the present phenomenological model is thus “predictable”. In fact, a similar approach for the $\text{Al}_2\text{O}_3\text{-CaO-MgO-SiO}_2$ quaternary slags was reported by Gan et al. [37] We have also tried to extend the modified VFT equation to the above quaternary slags. The results are similar to the $\text{Al}_2\text{O}_3\text{-CaO-SiO}_2$ ternary slags. Due to space limitations, the modified VFT model calculation results for the $\text{Al}_2\text{O}_3\text{-CaO-MgO-SiO}_2$ quaternary slags are not given here.

4. Application to TTT and CCT diagrams

In order to further verify the applicability of the present modified VFT equation, the isothermal time-temperature-transformation (TTT) and non-isothermal continuous-cooling-transformation (CCT) of the solid precipitations from the supercooled $\text{Al}_2\text{O}_3\text{-CaO-SiO}_2$ melts have been examined.

The classical Johnson-Mehl-Avrami-Kolmogorov (JMAK) equation [38,39], for spherical particles and isothermal transformation, has been used to calculate the isothermal time-temperature-transformation relation:

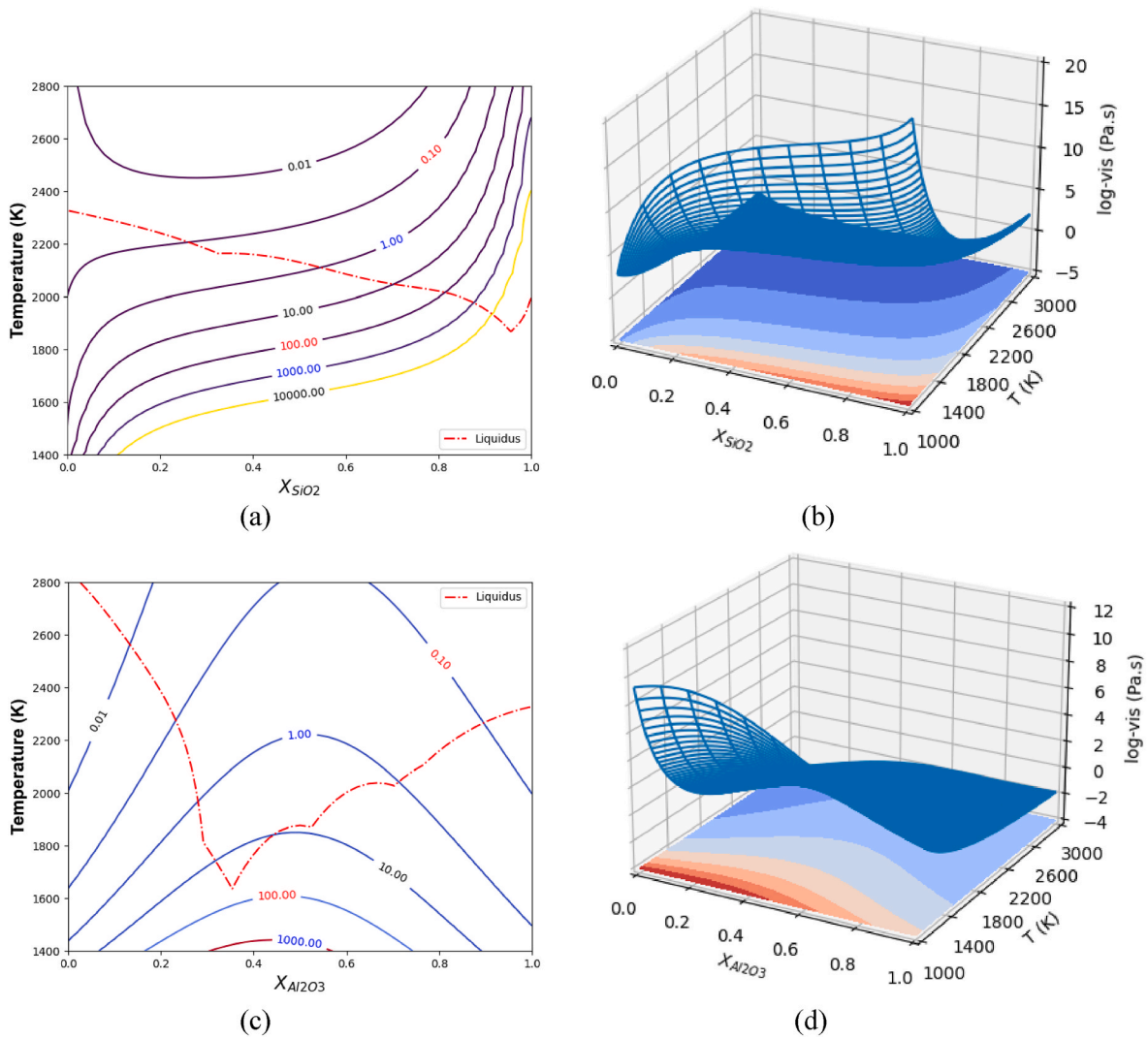


Fig. 4. Calculated the viscosity contours (Pa.s) in (a) the $\text{Al}_2\text{O}_3\text{-SiO}_2$ and (c) $\text{Al}_2\text{O}_3\text{-CaO}$ binary slags with liquidus boundaries. The corresponding 3d-plot for the composition-temperature-viscosity relations in (b) $\text{Al}_2\text{O}_3\text{-SiO}_2$ and (d) $\text{Al}_2\text{O}_3\text{-CaO}$ binary slags.

$$X(t) = 1 - \exp\left\{-\frac{\pi}{3}N_r G_r^3 t^n\right\} \quad (5)$$

where $X(t)$ is the volume fraction transformed at time t . N_r is the nucleation rate, and G_r is the growth rate. n is the Avrami number, which varies from 1 to 4. For the slag system, we assume the initial solid precipitate is sphere, so we set $n = 4$. In this work, the thresholds of beginning and finishing crystallization are set to be 0.01 and 0.99, respectively. A similar approach was used in determination of the isothermal TTT curves of solid phases from molten slags by Nassyrov and Jung [40].

In order to successful calculate the TTT curve of solid phase, the above equations rely on the ability to calculate both nucleation and growth rates. The nucleation rate, N_r , follows the suggestion by Saunders and Miodownik [41,42], is calculated by introducing an effective wetting angle, θ , for the heterogenous nucleation:

$$N_r = \frac{N_0 D_e}{a_0^2} \exp\left[-\frac{16\pi}{3N_A kT} f(\theta) \frac{\alpha^3 \cdot \Delta H_m^3}{\Delta G_m^2}\right] \quad (6)$$

where N_0 is the number of potential sites for nucleation, D_e is the effective diffusivity coefficient, a_0 is an atomic spacing, G^* is the Gibbs energy barrier to nucleation, k is Boltzman's constant, N_A is Avagadro's number, α is a constant relating to the matrix/nucleus interfacial energy

suggested by Turnbull [43], and ΔH_m and ΔG_m are the enthalpy and molar Gibbs energy driving force of phase transformation, respectively. In the present work, a VBA code has been developed based on the quasichemical cell model [44] for the calculation of ΔG_m for a given $\text{Al}_2\text{O}_3\text{-CaO-SiO}_2$ slag. The ΔH_m is then calculated based on the Gibbs-Helmholtz relation. The $f(\theta)$ is expressed as: $f(\theta) = (2-3\cos\theta + \cos^3\theta)/4$. The value of θ can be determined using the experimental nose temperature, a minimum transformation time at a single temperature.

The growth rate can be expressed as:

$$G_r = \kappa D_e \frac{\Delta G_m}{RT} \quad (7)$$

where κ is the growth constant. In the present work, this parameter is determined by the experimental TTT relation. If there are sufficient TTT relations for the solid precipitate phases, this parameter can also be treated as a function of slag composition.

The effective diffusion coefficient, D_e , plays a significant role in both the nucleation and growth rate. In the present work, the absolute rate theory proposed by Eyring [45] has been applied to estimate the ionic diffusivity:

$$D_i = \frac{kT}{\eta\lambda_i} \quad (8)$$

here λ_i is the ionic diameter. The values of Al^{3+} , Ca^{2+} , Si^{4+} and O^{2-} ionic diameters were taken from the literature [46]. The effective diffusivity of a given slag can then be determined by:

$$D_e = \left[\sum_{i=1}^4 \frac{1}{D_i} \right]^{-1} \quad (9)$$

where i represents different ions. The inverse of the diffusion coefficients for different ions are added so that the ion with the slowest diffusion rate gets the most weight. A preliminary investigation has confirmed that Eq. (9) gives reasonable agreement with the experimental values in the Al_2O_3 - CaO - SiO_2 slags.

Eq (8) is actually a similar form of the well-known Einstein-Stokes equation [45], for the diffusion of spherical particles through a liquid with low Reynolds numbers. Once the effective diffusivity has been determined, both the nucleation and growth rates at a given temperature for a given slag can thus be defined. The incubation time for isothermal transformation can thus be defined.

For effective controlling of the precipitates during slag solidification, the so-called continuous cooling transformation (CCT) relation is generally more appropriate for engineering application. Because slags are normally cooled from a processing temperature with either natural cooling or controllable rate. Since the TTT relation of a given solid precipitate has been determined, the Scheil additivity rule [47] can be applied to determine the transformation kinetics when the slag is cooled with an arbitrary cooling rate. The additivity rule is considered as a special algorithm for predicting the non-isothermal transformations on the basis of known isothermal kinetic data. The mathematical expression [48] of the additivity hypothesis is:

$$\int_0^{t_x} \frac{dt}{\tau_x(T)} = av^b \quad (10)$$

$\tau_x(T)$, the incubation time at temperature T and fraction of x transformed, is given by the TTT relation. t_x is the time to reach x fraction at a cooling rate v . a and b are the constants. If there is no experimental CCT relation available, it is generally set the value of av^b to unity [49].

Numerically discretization of the integral form of additivity rule by n steps in Eq (10), we obtain the following calculation relationship:

$$\sum_{i=1}^n \frac{\Delta t_i}{\tau_i} = 1 \quad (11)$$

where Δt_i is the time period for the i th isothermal step at temperature T_i ; and τ_i is the isothermal incubation time at T_i .

Cramb [50] reported the TTT and CCT relations for three Al_2O_3 - CaO binary slags measured by the double hot thermocouple technique (DHTT). Fig. 5 shows the calculated TTT and CCT relations for the solid CaAl_2O_4 phase crystallized from Slag A (51.47% Al_2O_3 -48.53% CaO). The melting temperature of this slag is calculated using the FactSage FToxid commercial database [31]. As shown in Fig. 5, the undercooling temperature for the solidification of CaAl_2O_4 is higher than 70 °C, depending upon the cooling rate. The non-isothermal CCT relation indicates an even higher undercooling degree is required in comparison with the isothermal TTT relation. Although there are several factors in the JMAK equation that affect the TTT relation (and later additivity hypothesis for the CCT relation), the effective diffusivity determined by the viscosity is one of the key factors. A preliminary examination of the influence of effective diffusivity on the TTT relation has been examined in this work. It will primarily shift the incubation time to a higher range if the viscosity is about 15% higher than the accessed values.

Rocabois et al. [51] reported the TTT relation for anorthite primary phase crystallized from a 24.5% Al_2O_3 -33.7% CaO -41.3% SiO_2 -0.25% MgO slag. Since the MgO content was rather lower, it can be approximated as the ternary Al_2O_3 - CaO - SiO_2 slag. Fig. 6 shows the calculated TTT relations in comparison with the experimental results. The

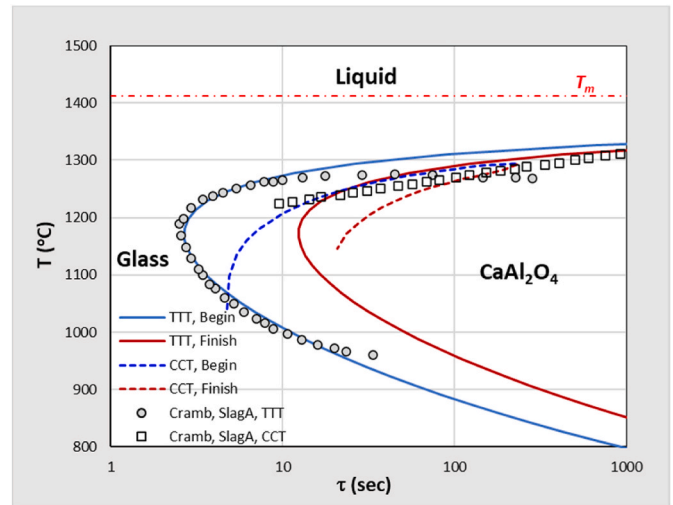


Fig. 5. Calculated initial and final TTT and CCT curves of CaAl_2O_4 solid phase in a 51.47% Al_2O_3 -48.53% CaO slag.

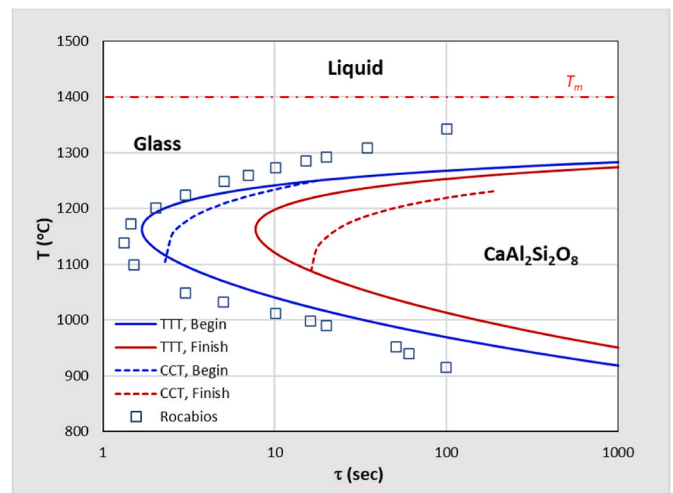


Fig. 6. Calculated initial and final TTT and CCT relations of $\text{CaAl}_2\text{Si}_2\text{O}_8$ precipitated from a 24.5% Al_2O_3 -33.7% CaO -41.3% SiO_2 -0.25% MgO slag.

calculated TTT curve for the beginning crystallization of $\text{CaAl}_2\text{Si}_2\text{O}_8$ (anorthite) phase is in good agreement with the experimental data. The finished crystallization TTT and CCT curves are calculated by the JMAK model and additivity rule. Rocabois co-authored with Lehmann and Gaye [52] and developed a kinetic model for the precipitation of non-metallic inclusions in steels. They found that the calculated compositions of oxide inclusions differ from those of inclusions precipitating at equilibrium. The present modelling results give the similar results, i.e. CCT curves of solid phases do not agree with the equilibrium calculation results.

5. Conclusion

A phenomenological viscosity model has been developed on the basis of modification of the VFT equation. Similar to the Calphad modelling, the VFT model parameters are expanded as the functions of composition and temperature. The model is used to calculate the viscosity of the Al_2O_3 - CaO - SiO_2 silicate system in the entire composition space and in a wide temperature range, from homogenous liquid to the heterogenous glass-transition temperature. Similar to the Calphad model, the modified VFT model is readily extended to calculate the viscosities of the higher-

order oxide systems. Application of the modified VFT viscosity models to simulate the isothermal TTT and non-isothermal CCT incubation time and temperature relationships of CaAl_2O_4 and $\text{CaAl}_2\text{Si}_2\text{O}_8$ solid precipitated phases have been carried out. The simulation results fit well with the experimental data reported in the literature. The TTT and CCT diagram calculations verify the reliability of the phenomenological viscosity model.

Declaration of competing interest

The authors declare that they have no known competing financial interests or personal relationships that could have appeared to influence the work reported in this paper.

Acknowledgment

The current work has received funding from the European Union's Horizon 2020 research and innovation program under grant agreement No 869268 (Sisal Pilot) and No 767533 (EnsureAI).

References

- [1] C. Liu, S. Huang, B. Blanpain, M. Guo, Optimization of mineralogy and microstructure of solidified basic oxygen furnace slag through SiO_2 addition or atmosphere control during hot-stage slag treatment, *Metall. Mater. Trans. B* 50 (1) (2019) 210–218.
- [2] Y. Sun, Z. Zhang, L. Liu, X. Wang, Heat recovery from high temperature slags: a review of chemical methods, *Energies* 8 (3) (2015) 1917–1935.
- [3] M. Barati, S. Esfahani, T. Utigard, Energy recovery from high temperature slags, *Energy* 36 (9) (2011) 5440–5449.
- [4] M. Campforts, B. Blanpain, P. Wollants, The importance of slag engineering in freeze-lining applications, *Metall. Mater. Trans. B* 40 (5) (2009) 643–655.
- [5] A.W. Cramb, The solidification behavior of slags: phenomena related to mold slags, *ISIJ Int.* 54 (12) (2014) 2665–2671.
- [6] J. Miller, A. Irgens, Alumina production by the Pedersen process—history and future, in: *Essential Readings in Light Metals*, Springer, 2016, pp. 977–982.
- [7] J. Safarian, L. Kolbeinsen, Sustainability in Alumina Production from Bauxite, *Sustainable Industrial Processing Summit*, 2016, pp. 75–82.
- [8] P.C. Pistorius, C. Coetzee, Physicochemical aspects of titanium slag production and solidification, *Metall. Mater. Trans. B* 34 (5) (2003) 581–588.
- [9] C.A. Angell, K.L. Ngai, G.B. McKenna, P.F. McMillan, S.W. Martin, Relaxation in glass-forming liquids and amorphous solids, *J. Appl. Phys.* 88 (6) (2000) 3113–3157.
- [10] S. Vargas, F. Frandsen, K. Dam-Johansen, Rheological properties of high-temperature melts of coal ashes and other silicates, *Prog. Energy Combust.* 27 (3) (2001) 237–429.
- [11] T. Iida, H. Sakai, Y. Kita, K. Shigeno, An equation for accurate prediction of the viscosities of blast furnace type slags from chemical composition, *ISIJ Int.* 40 (Suppl) (2000) S110–S114.
- [12] P.V. Riboud, Y. Roux, L.D. Lucas, H. Gaye, Improvement of continuous casting powders, *Fachber. Hüttenprax. Metallweiterverarb.* 19 (8) (1981) 859–869.
- [13] Tang, K. and M. Tangstad, *Modeling viscosities of ferromanganese slags*, in *INFACON XI 2007*: New Delhi, India.
- [14] A.N. Grundy, H. Liu, I. Jung, S.A. Decterov, A.D. Pelton, A model to calculate the viscosity of silicate melts, *Int. J. Mater. Res.* 99 (11) (2008) 1185–1194.
- [15] L. Zhang, S. Jahanshahi, Review and modeling of viscosity of silicate melts: Part I. Viscosity of binary and ternary silicates containing CaO, MgO, and MnO, *Metall. Mater. Trans. B* 29 (1) (1998) 177–186.
- [16] A. Costa, Viscosity of high crystal content melts: dependence on solid fraction, *Geophys. Res. Lett.* 32 (22) (2005).
- [17] H. Vogel, Das temperaturabhängigkeitsgesetz der viskosität von flüssigkeiten, *Phys. Z.* 22 (1921) 645–646.
- [18] G.S. Fulcher, Analysis of recent measurements of the viscosity of glasses, *J. Am. Ceram. Soc.* 8 (6) (1925) 339–355.
- [19] G. Tammann, W. Hesse, Die Abhängigkeit der Viskosität von der Temperatur bei unterkühlten Flüssigkeiten, *Z. Anorg. Allg. Chem.* 156 (1) (1926) 245–257.
- [20] J.C. Mauro, Y.Z. Yue, A.J. Ellison, P.K. Gupta, D.C. Allan, Viscosity of glass-forming liquids, *Proc. Natl. Acad. Sci. USA* 106 (47) (2009) 19780–19784.
- [21] P.G. Debenedetti, F.H. Stillinger, Supercooled liquids and the glass transition, *Nature* 410 (6825) (2001) 259–267.
- [22] K. Hu, K. Tang, X. Lv, J. Safarian, Z. Yan, B. Song, Modeling viscosity of high titania slag, *Metall. Mater. Trans. B* (2020) 1–10.
- [23] *Slag Atlas*, 2nd Revised edition, VDEh, Verlag Stahleisen GmbH, 1995.
- [24] J. Russell, D. Giordano, D. Dingwell, High-temperature limits on viscosity of non-Arrhenian silicate melts, *Am. Mineral.* 88 (8–9) (2003) 1390–1394.
- [25] D.R. Neuville, Viscosity, structure and mixing in (Ca, Na) silicate melts, *Chem. Geol.* 229 (1–3) (2006) 28–41.
- [26] A. Sipp, Y. Bottinga, P. Richet, New high viscosity data for 3D network liquids and new correlations between old parameters, *J. Non-Cryst. Solids* 288 (1–3) (2001) 166–174.
- [27] D. Sifakas, T. Matsushita, S. Hakamada, K. Onodera, F. Kargl, A.E. Jarfors, M. Watanabe, Measurement of viscosity of SiO_2 -CaO- Al_2O_3 slag in wide temperature range by aerodynamic levitation and rotating bob methods and sources of systematic error, *Int. J. Microgr. Sci. Appl.* 35 (2) (2018), 350204.
- [28] D. Sifakas, T. Matsushita, A.E.W. Jarfors, S. Hakamada, M. Watanabe, Viscosity of SiO_2 -CaO- Al_2O_3 slag with low silica-influence of CaO/ Al_2O_3 , SiO_2 / Al_2O_3 ratio, *ISIJ Int.* 58 (12) (2018) 2180–2185.
- [29] M.J. Toplis, D.B. Dingwell, Shear viscosities of CaO- Al_2O_3 - SiO_2 and MgO- Al_2O_3 - SiO_2 liquids: implications for the structural role of aluminium and the degree of polymerisation of synthetic and natural aluminosilicate melts, *Geochem. Cosmochim. Acta* 68 (24) (2004) 5169–5188.
- [30] S.L. Webb, M. Banaszak, U. Köhler, S. Rausch, G. Raschke, The viscosity of Na₂O-CaO- Al_2O_3 - SiO_2 melts, *Eur. J. Mineral* 19 (5) (2007) 681–692.
- [31] C. Bale, E. Bélice, P. Chartrand, S. Decterov, G. Eriksson, K. Hack, I.-H. Jung, Y.-B. Kang, J. Melançon, A. Pelton, FactSage thermochemical software and databases—recent developments, *Calphad* 33 (2) (2009) 295–311.
- [32] R.A. Blomquist, J.K. Fink, L. Leibowitz, *THE VISCOSITY OF MOLTEN ALUMINA*, Argonne National Laboratory, Argonne, Illinois, 1978.
- [33] P. Kozakevitch, Viscosité et éléments structuraux des aluminosilicates fondus : laitiers CaO- Al_2O_3 - SiO_2 entre 1600-2100°C, *Rev. Métall.* 57 (2) (1960) 149–160.
- [34] G. Hofmaier, Berg Huttenm. Monatsh. Montan. Hochschule Loebnig 113 (1968) 270–281.
- [35] G. Urbain, Y. Bottinga, P. Richet, Viscosity of liquid silica, silicates and aluminosilicates, *Geochem. Cosmochim. Acta* 46 (6) (1982) 1061–1072.
- [36] J.C. Mauro, A.J. Ellison, D.C. Allan, M.M. Smedskjaer, Topological model for the viscosity of multicomponent glass-forming liquids, *Int. J. Appl. Glass Sci.* 4 (4) (2013) 408–413.
- [37] L. Gan, J. Xin, Y. Zhou, Accurate viscosity calculation for melts in SiO_2 - Al_2O_3 -CaO-MgO systems, *ISIJ Int.* 57 (8) (2017) 1303–1312.
- [38] D.R. Uhlmann, A kinetic treatment of glass formation, *J. Non-Cryst. Solids* 7 (4) (1972) 337–348.
- [39] K. Barmak, A commentary on: “reaction kinetics in processes of nucleation and growth”, *Metall. Mater. Trans. B* 49 (6) (2018) 3616–3680.
- [40] D. Nassyrov, I.-H. Jung, in: *A Model for Slag Solidification*, Association for Iron & Steel Technology, 2014.
- [41] N. Saunders, A. Miodownik, Evaluation of glass forming ability in binary and ternary metallic alloy systems—an application of thermodynamic phase diagram calculations, *Mater. Sci. Technol.* 4 (9) (1988) 768–777.
- [42] A. Miodownik, N. Saunders, Modelling of materials properties in duplex stainless steels, *Mater. Sci. Technol.* 18 (8) (2002) 861–868.
- [43] D. Turnbull, Formation of crystal nuclei in liquid metals, *J. Appl. Phys.* 21 (10) (1950) 1022–1028.
- [44] H. Gaye, J. Lehmann, T. Matsumiya, W. Yamada, A statistical thermodynamics model of slags: applications to systems containing S, F, P₂O₅ and Cr oxides, in: *4th International Conference on Molten Slags and Fluxes*, 1992.
- [45] H. Eyring, Viscosity, plasticity, and diffusion as examples of absolute reaction rates, *J. Chem. Phys.* 4 (4) (1936) 283–291.
- [46] R.D. Shannon, Revised effective ionic radii and systematic studies of interatomic distances in halides and chalcogenides, *Acta Crystallogr. Sect. A Cryst. Phys. Diff. Theor. Gen. Crystallogr.* 32 (5) (1976) 751–767.
- [47] J.W. Cahn, Transformation kinetics during continuous cooling, *Acta Metall.* 4 (6) (1956) 572–575.
- [48] T. Hsu, Additivity hypothesis and effects of stress on phase transformations in steel, *Curr. Opin. Solid State Mater. Sci.* 9 (6) (2005) 256–268.
- [49] F. Liu, C. Yang, G. Yang, Y. Zhou, Additivity rule, isothermal and non-isothermal transformations on the basis of an analytical transformation model, *Acta Mater.* 55 (15) (2007) 5255–5267.
- [50] A.W. Cramb, *Quantifying the Thermal Behavior of Slags (TRP 9903)*, American Iron and Steel Institute (US), 2003.
- [51] P. Rocobois, J. Pontoire, J. Lehmann, H. Gaye, Crystallization kinetics of Al_2O_3 -CaO- SiO_2 based oxide inclusions, *J. Non-Cryst. Solids* 282 (1) (2001) 98–109.
- [52] J. Lehmann, P. Rocobois, H. Gaye, Kinetic model of non-metallic inclusions' precipitation during steel solidification, *J. Non-Cryst. Solids* 282 (1) (2001) 61–71.